Second Conference on Smart Monitoring,
Assessment and Rehabilitation of Civil Structures

SMAR 2013

Performance of axially loaded concrete cylinders confined with SFRP materials

C. Faella[1], A. Napoli[1], and R. Realfonzo[1]

[1] Department of Civil Engineering, University of Salerno, Fisciano (SA), Italy

ABSTRACT: The paper presents the first results of a wide experimental campaign performed to investigate the compressive behaviour of plain concrete cylinders (150 mm diameter and 300 mm height) confined with Steel Fiber Reinforced Polymer (SFRP) materials. The complete test matrix includes 252 specimens and the main parameters investigated were the target compressive strength of the unconfined concrete (8, 15, 30 and 35 MPa) and the number of SFRP layers used for column jacketing (1, 2, and 3). Tests presented herein are 49, all belonging to the 15MPa-series, and the obtained results have allowed to investigate the effectiveness of using SFRP confining system to increase the compressive strength and ductility of concrete. Other aspects investigated herein deal with the stress-strain behavior, the circumferential strains of the SFRP jacket and the failure modes of SFRP wrapped specimens.

1 INTRODUCTION

In existing framed buildings, the external confinement of reinforced concrete (RC) columns with Fiber Reinforced Polymer (FRP) materials is being used in place of more traditional strengthening techniques, such as steel or concrete jacketing. Typically, FRP confinement systems employ carbon (CFRP), glass (GFRP) and aramid (AFRP) fibers. The effectiveness of using these materials has been widely investigated in the literature, and a number of analytical models to predict the compressive behaviour of FRP confined concrete have been proposed; advanced states of the art on these topics can be found in literature (Teng et al. 2002, Realfonzo and Napoli 2011, Napoli and Realfonzo 2011).

Recently, a new class of composites made of steel FRP (SFRP) sheets has emerged as a promising and cost-effective solution for external confinement of RC members. The SFRP sheet consists of high carbon steel cords made by twisting steel wires instead of carbon/glass fibers; it can be applied via wet lay-up by using epoxy resin. Alternatively, the sheet can be impregnated with special mortars to realize a strengthening system known with the acronym of SFRG ("Steel Fiber Reinforced Grout"). Despite the non-flexible nature of the SFRP sheet which makes the column wrapping relatively difficult in comparison to CFRP or GFRP applications, this composite material is expected to exhibit a superior behavior due to the high properties of the steel cords constituting the single layer. In fact, preliminary investigations performed by Mashrik (2011) have proven that the increase of compressive strength and ductility achievable with SFRP confinement is greater than that obtained with the CFRP system. Also, the SFRP system seems to provide a better response in presence of aggressive environmental exposures.

To date, the literature related to SFRP confined concrete is rather limited. Only recently, few researchers have experimentally investigated the effectiveness of this strengthening system by performing compression tests on small scale (El-Hacha and Mashrik 2012) or large scale SFRP confined columns (Abdelrahman and El-Hacha 2012). Later, Napoli et al. (2013) have examined the performance of full scale reinforced concrete columns strengthened with SFRP and subjected to cyclic flexure under a constant axial load.

With the aim to deepen the knowledge on the compressive behaviour of concrete confined by SFRP, a wide experimental campaign is in progress at the Laboratory of Material and Structural Testing of the University of Salerno (Italy). The test matrix includes 252 small scale plain concrete circular specimens (150 mm diameter by 300 mm height) that were grouped in four series according to the target compressive strength of the unconfined concrete, f_{c0} (8, 15, 30 and 35 MPa). Most specimens were variably confined by using 1, 2 or 3 layers of SFRP sheets characterized by different steel fiber densities (low, medium and high); the remaining ones were not strengthened and used as reference (control) members. This paper focuses on the first 49 of 94 compressive tests performed on specimens belonging to the 15MPa-series, and the obtained results have allowed to preliminary investigate the performance of SFRP confined specimens in terms of axial strength and ductility.

2 EXPERIMENTAL PROGRAM

As mentioned earlier, the 49 concrete specimens considered in this paper are characterized by a target compression strength of the unconfined concrete, f_{c0}, equal to 15 MPa. This low value for f_{c0} is frequently found in existing buildings where retrofitting by SFRP confinement may be needed. Of these members, 13 were used as control (unstrengthened) specimens, whereas the remaining ones (36) were variably confined by employing 1, 2 or 3 SFRP layers characterized by equal or different steel fiber densities (low, medium or high). The following sections provide a detailed description about SFRP materials, strengthening layouts, set-up and instrumentation.

2.1 SFRP materials and strengthening layouts

The SFRP sheets employed in the experimental campaign were type "Fidsteel 3x2-B *y*-12 Hardwire™" (2012). The first two digits (3x2) indicate the type of hardwire cord, which is made by twisting five individual wire filaments together - three straight filaments wrapped by two filaments at a high twist angle. The third digit (B *y*) indicates the tape density, i.e. the number of wires per inch (= 25,4 mm). In this study, SFRP sheets with three different densities were selected, labeled B4 (= 4 wires/25.4 mm), B12 (= 12 wires/25.4 mm) and B20 (= 20 wires/25.4 mm), and classified herein as low (LD), medium (MD), and high density (HD), respectively (Fig. 1). The final digit refers to the width of the sheet which is equal to 12 inch (305 mm). Table 1 provides the thickness and mechanical properties of these materials, as provided by the supplier, where: t_s is the sheet equivalent design thickness; f_s the ultimate tensile strength; E_s the elastic modulus and $\varepsilon_{s,u}$ the ultimate strain.

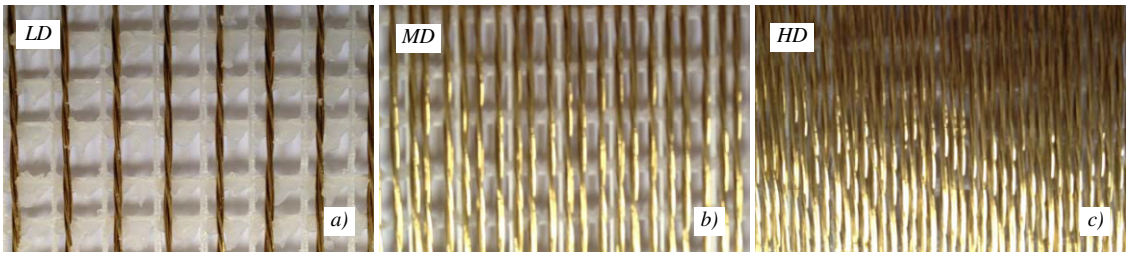

Figure 1. SFRP sheets with low (a), medium (b) and high (c) density.

Table 1. Thickness and mechanical properties of SFRP sheets.

Hardwire™ steel fiber	density	t_s mm	f_s MPa	E_s GPa	$\varepsilon_{s,u}$ %
FIDSTEEL 3x2-B4	Low (LD)	0.075			
FIDSTEEL 3x2-B12	Medium (MD)	0.227	3070	190	1.60
FIDSTEEL 3x2-B20	High (HD)	0.378			

Fidsaturant HM-T (2012) epoxy adhesive was used to bond the SFRP sheets around the specimens. It is a two-component thixotropic epoxy characterized by a tensile strength of 70 MPa, an elasticity modulus of 2500 MPa and an elongation at rupture of 6%.

Single or multiple SFRP layers with equal or different densities were combined in order to obtain confining systems with varying elastic stiffness (k_{conf}) given by:

$$k_{conf} = \frac{2 \cdot t_j \cdot E_s}{D} \tag{1}$$

where t_j is the total stiffness of the SFRP, and D is the cylinder diameter (=150 mm).

Table 2 reports the 18 strengthening layouts (*S1* to *S18*) investigated in the complete experimental program, and the 12 configurations considered in this paper are highlighted in grey background. As noted, they range from one layer of low density sheet ("1LD") to three layers made of medium (one layer) and high (two layers) density sheets ("1MD+2HD"). These two boundary configurations give rise to the lowest and highest stiffness of the confining system, equal to 185 MPa and 2400 MPa, respectively. In the case of multiple SFRP layers, an overlap length of about 200 mm (≈ half circumference) was considered; this value is approximately twice the minimum length recommended by Mashrik (2011) to avoid a premature debonding failure of the SFRP wrap at the overlap zone.

Table 2. Strengthening layout.

S1	*S2*	*S3*	*S4*	*S5*	*S6*	*S7*	*S8*	*S9*
1LD	1MD	1HD	2LD	2MD	2HD	3LD	3MD	3HD
S10	*S11*	*S12*	*S13*	*S14*	*S15*	*S16*	*S17*	*S18*
1LD +1MD	1LD +1HD	1MD +1HD	2LD+1MD	2LD+1HD	2MD+1HD	1LD+2MD	1LD+2HD	1MD+2HD

2.2 Set-up and instrumentation

Specimens were subjected to a monotonic concentric uniaxial compression load applied in displacement control at a rate of 2mm/min. Tests were stopped at the achievement of a 40% load decay evaluated with respect to the peak value recorded for each specimen. The set-up is shown in Figure 2a. To ensure horizontal and smooth surfaces at both ends of the specimens for uniform loading, the top and bottom faces of the cylinders were capped with sulfur.

During tests, four wire transducers monitored the vertical displacement imposed to the specimen and checked the perfect horizontality of the top and bottom plates of the testing machine (see Fig. 2a). Also, a number of strain gauges were used to measure circumferential and vertical strains of both unconfined and SFRP confined concrete. In particular, the unconfined specimens were instrumented with three vertical and three horizontal strain gauges at the mid-height located 120° apart to measure the axial and hoop strains, respectively. The same configuration was also used for most of the SFRP confined specimens (Fig. 2b), whereas for other members the number of horizontal strain gauges was doubled (from 3 to 6).

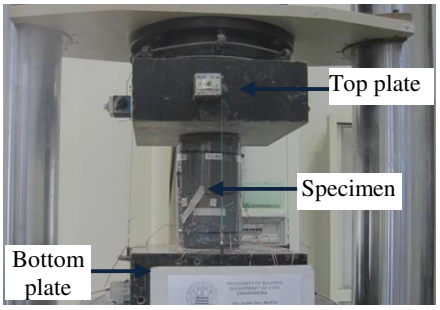

a)

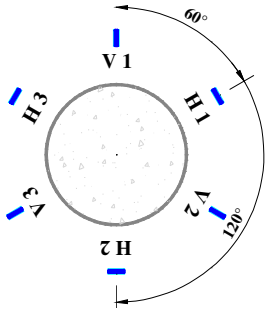

b)

Figure 2. Testing frame (a), and strain gauge distribution (b).

3 EXPERIMENTAL RESULTS AND DISCUSSION

Table 3 summarizes main data and results of the 49 compression tests performed so far; a set of three tests per SFRP configuration was carried out. Each test is identified by a label providing information on: *a)* type of SFRP strengthening layout among those of Table 2 (ranging from S1 to S18); *b)* identification number of the specimen within each set of analogous members (ranging from #1 to #3). In the Table, the first 13 tests (designed with labels spanning from S0#1 to S0#13) identify the unconfined members: of these, five cylinders were tested in axial compression with the aim to obtain the whole axial stress-strain law of the unconfined concrete; the remaining ones, instead, were only tested to know the respective compression strengths. For each test, Table 3 also provides: the total thickness (t_j) and elastic stiffness (k_{conf}) of the employed SFRP jacket; diameter (Ø) and height (H) of the cylinder; the peak compressive strength of the unconfined (f_{co}) or SFRP confined concrete (f_{cc}); the respective average ($f_{co,av}$; $f_{cc,av}$) and standard deviation (σ_{fco}; σ_{fcc}) values resulting from each test set; the normalized value of f_{cc} with respect to $f_{co,av}$; the axial strain of the unconfined or SFRP confined concrete corresponding to the peak strength (ε_{co} and ε_{cc}, respectively) and the respective values of the average ($\varepsilon_{co,av}$; $\varepsilon_{cc,av}$) and standard deviation ($\sigma_{\varepsilon co}$; $\sigma_{\varepsilon cc}$); the $\varepsilon_{cc}/\varepsilon_{co,av}$ ratio; the ultimate strain of the unconfined (ε_{cu}) or SFRP confined concrete (ε_{ccu}). It is highlighted that the experimental values of the axial strains have been computed by the ratio between the displacement imposed by the testing machine and the initial height of the specimen. From the table it is noted that for SFRP confined specimens ε_{cc} generally coincides with the ultimate strain ε_{ccu}; however, when this matching is not verified, the ultimate condition is reached for values of ε_{ccu} very close to ε_{cc}.

The following sections provide a preliminary discussion of the results obtained so far in terms of peak compression strength and strain, stress-strain response, circumferential strain of the SFRP jacket and failure modes of the SFRP wrapped specimens.

3.1 Compressive strength and corresponding strain of the SFRP confined concrete

As already observed for CFRP or GFRP confined specimens (Realfonzo et al. 2011, Napoli et al. 2011), the results reported in Table 3 highlight, except for some test sets, a higher scatter of data in terms of axial strains; this evidence obviously affects the development of reliable predictive models. By focusing on the strengthening layouts S1 to S6, it is noted that doubling the number of SFRP layers with same fiber density (2LD, 2MD, or 2HD) a strength increase of about 50% is obtained. This evidence confirms what already found by El-Hacha and Mashrik (2012); they noted that doubling the number of SFRP layers, the resulting percent increase in strength is not doubled or tripled, i.e. number of layers and increase of strength are not linearly related. Similar percent increases are also calculated in terms of axial strains, except in the case of specimens "type S4" for which only slight improvements are observed.

Table 3. Test results.

Test	t_j	k_{conf}	Ø	H	f_{cc} (f_{co})	$f_{cc,av}$ ($f_{co,av}$)	σ_{fcc} (σ_{fco})	$f_{cc}/f_{co,av}$	ε_{cc} (ε_{co})	$\varepsilon_{cc,av}$ ($\varepsilon_{co,av}$)	$\sigma_{\varepsilon cc}$ ($\sigma_{\varepsilon co}$)	$\varepsilon_{cc}/\varepsilon_{co,av}$	ε_{ccu} [1] (ε_{cu})
	mm	MPa	mm	mm	MPa	MPa	MPa	-	‰	‰	MPa	-	‰
S0#1	-	-	156.0	301	13.91			-	3.36			-	5.35
S0#2	-	-	154.6	322	16.12			-	3.13			-	6.04
S0#3	-	-	154.5	324	16.12			-	3.02			-	7.77
S0#4	-	-	154.5	320	11.88			-	3.64			-	3.64
S0#5	-	-	154.3	324	18.24			-	2.86			-	6.09
S0#6	-	-	155.0	-	15.20			-	-			-	-
S0#7	-	-	154.0	-	15.70	14.93	2.33	-	-	3.20	0.31	-	-
S0#8	-	-	155.0	-	18.30			-	-			-	-
S0#9	-	-	157.0	-	17.00			-	-			-	-
S0#10	-	-	155.0	-	12.20			-	-			-	-
S0#11	-	-	154.0	-	15.22			-	-			-	-
S0#12	-	-	154.0	-	13.04			-	-			-	-
S0#13	-	-	154.0	-	11.21			-	-			-	-
S1#1	0.08	185.1	154.0	318	32.74			2.19	16.51			5.16	*16.51*
S1#2	0.08	185.1	154.0	320	23.76	28.18	4.49	1.59	31.82	21.63	8.83	9.94	*31.82*
S1#3	0.08	185.1	154.0	323	28.04			1.88	16.56			5.17	*16.56*
S2#1	0.23	556.5	155.0	308	54.71			3.66	37.27			11.64	*37.27*
S2#2	0.23	560.1	154.0	323	46.64	49.61	4.44	3.12	38.38	35.47	4.12	11.99	*38.38*
S2#3	0.23	560.1	154.0	322	47.47			3.18	30.75			9.60	*30.75*
S3#1	0.38	919.0	156	323	65.48			4.38	50.27			15.70	*50.27*
S3#2	0.38	930.3	154	322	73.77	62.07	13.73	4.94	52.61	40.83	18.41	16.43	*52.61*
S3#3	0.38	925.5	155	323	46.96			3.14	19.61			6.13	22.15
S4#1	0.15	370.1	154.0	322	48.85			3.27	25.74			8.04	*25.74*
S4#2	0.15	370.1	154.0	322	45.71	45.02	4.22	3.06	22.39	23.41	2.03	6.99	*22.39*
S4#3	0.15	370.1	154.0	319	40.50			2.71	22.10			6.90	*22.10*
S5#1	0.45	1113.0	155.0	308	81.21			5.44	60.37			18.85	*60.37*
S5#2	0.45	1120.3	154.0	320	59.76	68.89	11.08	4.00	53.55	58.64	4.49	16.73	63.53
S5#3	0.45	1120.3	154.0	321	65.71			4.40	62.01			19.37	*62.01*
S6#1	0.76	1841.5	156.0	323	109.83			7.35	73.89			23.08	77.44
S6#2	0.76	1835.7	156.5	324	86.28	95.78	12.42	5.78	81.71	69.94	14.16	25.52	*81.71*
S6#3	0.76	1860.6	154.4	323	91.23			6.11	54.22			16.93	*54.22*
S10#1	0.30	740.4	155	322	51.97			3.48	29.31			9.15	*29.31*
S10#2	0.30	739.0	155.3	323	60.74	54.58	5.35	4.07	39.78	44.23	17.57	12.42	*39.78*
S10#3	0.30	738.0	155.5	324	51.03			3.42	63.59			19.86	*63.59*
S11#1	0.45	1117.8	154.0	302	63.96			4.28	86.01			26.86	*86.01*
S11#2	0.45	1128.0	152.6	320	64.94	54.46	17.30	4.35	44.16	54.26	28.09	13.79	50.28
S11#3	0.45	1109.1	155.2	322	34.49			2.31	32.61			10.18	49.91
S12#1	0.61	1478.5	155.5	326	82.19			5.50	59.51			18.59	*59.51*
S12#2	0.61	1474.7	155.9	323	77.71	79.95	2.24	5.20	44.70	62.57	19.58	13.96	47.87
S12#3	0.61	1482.3	155.1	323	79.96			5.35	83.49			26.08	*83.49*
S14#1	0.53	1290.3	155.5	323	78.66			5.27	61.97			19.35	*61.97*
S14#2	0.53	1298.6	154.5	323	74.41	72.94	6.59	4.98	42.16	66.14	26.31	13.17	*42.16*
S14#3	0.53	1282.0	156.5	324	65.74			4.40	94.28			29.45	*94.28*
S17#1	0.83	2024.2	156.0	307	98.66			6.61	79.40			24.80	86.41
S17#2	0.83	2055.9	153.6	324	89.57	95.25	4.96	6.00	57.61	68.33	10.89	17.99	59.89
S17#3	0.83	2022.9	156.1	325	97.53			6.53	67.99			21.24	68.67
S18#1	0.98	2419.3	154.4	323	122.03			8.17	75.13			23.46	*75.13*
S18#2	0.98	2406.8	155.2	320	110.00	118.93	7.85	7.37	80.62	78.13	2.78	25.18	*80.62*
S18#3	0.98	2405.3	155.3	324	124.76			8.35	78.64			24.56	*78.64*

[1] The values of $\varepsilon_{ccu} \equiv \varepsilon_{cc}$ are reported in italic

A further comparison can be made between the sets of specimens "type S5", confined with 2MD layers, and those "type S11" for which the same confinement stiffness k_{conf} was realized by combining 1LD+1HD layers; the cylinders "S11" have provided a significant data dispersion both in terms of strength and ductility and, on average, a reduced performance with respect to the counterparts "S5". However, this lower performance accounts for the results of the specimen S11#3 which experienced, during the test test, a premature debonding of the outer SFRP layer.

The efficiency of the SFRP confinement systems by varying the number and the type of SFRP layers can be better investigated by the bar charts in Figures 3a and 3b. In particular, in Figure 3a the strengthening layouts have been ordered based on the ascending values of the average strength increases $f_{cc,av}$ calculated, for each triplet of tests, with respect to the average value of the unconfined concrete strength $f_{cc,av.}$ Figure 3b, instead, shows a similar plot for the strain increases estimated in correspondence of the peak strength condition; these values have been obtained through the ratio, for each triplet of tests, between $\varepsilon_{cc,av}$ and $\varepsilon_{co,av.}$ values. It is observed that the strengths and corresponding strains of the SFRP wrapped specimens are much superior than the unwrapped members, thus highlighting the effectiveness of the SFRP confinement. The use of a single LD sheet (type S1), characterized by the lowest value of $k_{conf,}$, is sufficient by itself to almost double the peak compressive strength of the unconfined concrete, whereas the corresponding strain is more than six times over. The confinement with a SFRP system "type S18" (1MD+2HD), instead, characterized by the highest value of $k_{conf,}$ allows to provide performances in terms of strength and strain which are almost 8 and 25 times higher than those exhibited by the unconfined concrete. Looking at the distribution of the SFRP layouts based on the ascending values of strength and strain increases, it is noted that, except for particular cases, the performances improve with the stiffness of the confining system.

3.2 Stress-strain response

Figures 4a and 4b depict the comparison between the compressive behavior of a representative unconfined concrete member (namely S0#2) and the typical axial stress-strain curves of specimens wrapped with SFRP. In particular, Figure 4a shows the experimental curves of representative specimens confined with a single or two layers of SFRP sheets with equal fiber density (low, medium or high); Figure 4b, instead, refers to cylinders confined by combining multiple layers of SFRP sheets with different densities. As already observed in the case of CFRP or GFRP confining systems, the initial slope of the stress-strain curves of the SFRP wrapped specimens is very similar to that of unwrapped members, since the SFRP is not activated yet and most of the load is carried by concrete.

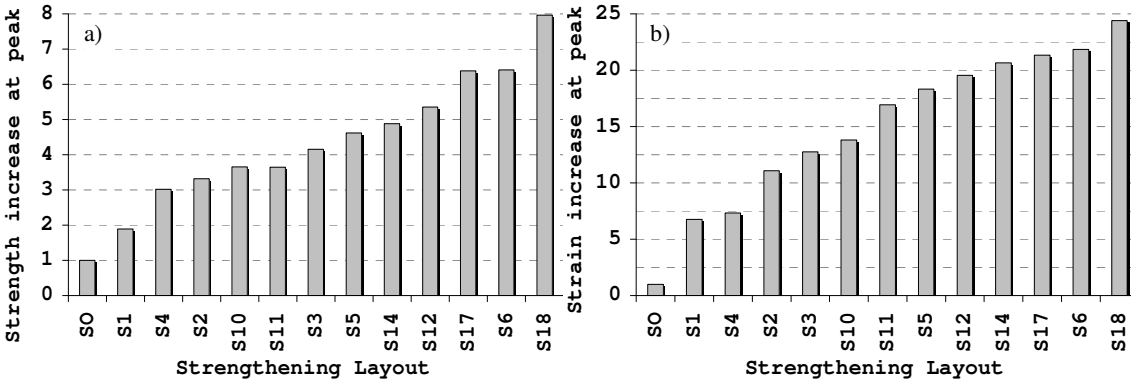

Figure 3. Average increases of strength (a) and strain (b) calculated with respect to the unconfined concrete.

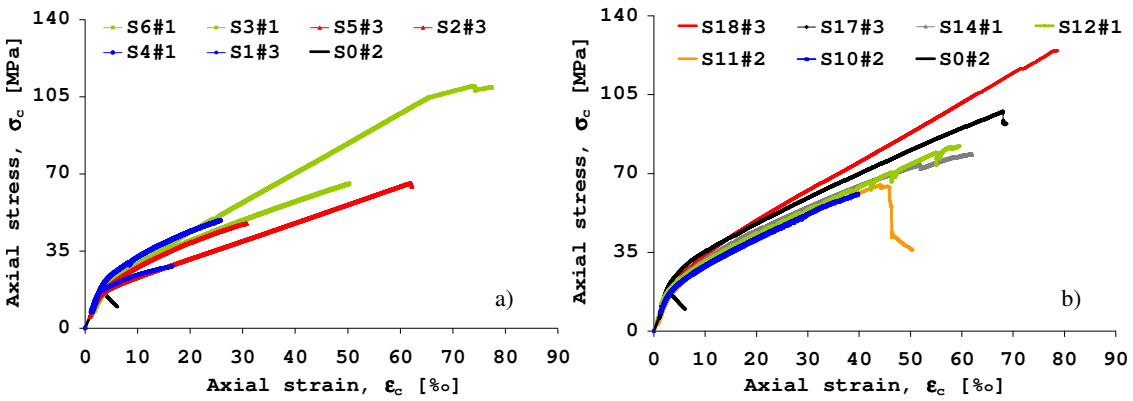

Figure 4. Typical axial stress-strain behavior for concrete confined with: different number of SFRP layers (a); multiple layers obtained by combining SFRP sheets with diverse densities (b).

Once the maximum load capacity achievable for an unconfined concrete is attained, the contribution of the SFRP jacket starts to become effective and, then, an almost elastic ascending branch characterizes the behavior of the confined concrete up to failure. The drop strength observed in the case of the specimen S11#2 is due to the debonding of the outer SFRP layer and then to the rupture of the inner one. Finally, Figure 4a clearly shows that the compressive behavior of the confined concrete significantly improves with increasing the number of SFRP layers. This can be clearly motivated since the confinement action depends on the radial pressure provided to the concrete core by the SFRP wraps. Increasing the number of SFRP layers enhances the stiffness of the confining wrap, and thus the radial pressure imposed on the concrete core, resulting in a greater increase in strength.

The effectiveness of the SFRP confining systems can be also investigated by analyzing the axial stress-circumferential strain responses plotted in Figure 5; they refer to specimens S1#1 and S4#2, confined with 1 and 2 layers of LD sheet, respectively. As mentioned earlier, such strains have been measured through three gauges located at the mid-height of the cylinders (120° apart). As already found by El-Hacha and Mashrik (2012), the curves are characterized by two linear ascending branches connected by a non-linear transition zone where the concrete is losing load carrying capacity and the SFRP is not fully activated yet. Also, it is observed that the average value of the maximum strains measured during the test S1#1 is about 1.2% which is quite close to the ultimate SFRP strain value provided by the supplier (= 1.6%); however it is highlithed that such average strain may account for lower values measured by strain gauges placed at the overlap region of the SFRP, i.e. where the sheet has double thickess.

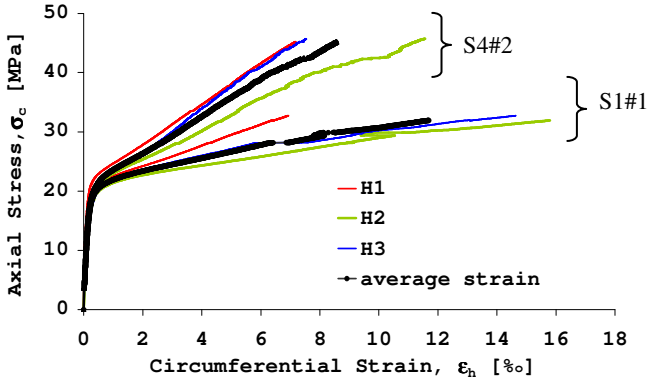

Figure 5. Axial stress-circumferential strain response for specimens S1#1 and S4#2.

3.3 Failure mode

Figure 6 depicts the typical failure modes exhibited by SFRP confined members. In particular, most specimens have experienced the rupture of the sheet right at the beginning of the overlap zone; the rupture involved the entire height of the cylinder (see Fig. 6a) or smaller portions. In a few cases, the rupture of the sheet was anticipated by severe damage of the fibers. Some specimens wrapped with multiple layers showed a combination of rupture and debonding. The debonding first occurred by involving the outer SFRP layer and was followed by the rupture of the inner layer/s which engaged half or the entire height of the cylinder (Fig. 6b). Only for the specimen S3#2 the sheet debonded at the overlap zone completely without rupture (Fig. 6c).

Figure 6. Typical failure modes of SFRP confined specimens.

4 CONCLUSIONS

The paper presented the first results of compression tests performed on plain concrete cylinders confined with SFRP wraps. It has been shown that the use of a single low density- SFRP layer, is sufficient by itself to almost double the strength of the unconfined concrete, whereas the corresponding strain is more than six times over. The use of 3 layers, obtained by combining SFRP sheets with medium and high density, provided performances in terms of strength and strain which are almost 8 and 25 times higher than those exhibited by the unconfined concrete.

5 ACKNOWLEDGMENTS

The Authors gratefully acknowledge “Fidia S.r.l. - Technical Global Services, Perugia, Italy” for financially supporting the experimental program and realizing the SFRP confining systems.

6 REFERENCES

Abdelrahman, K, and El-Hacha, R. 2012. Behavior of Large-Scale Concrete Columns Wrapped with CFRP and SFRP Sheets. *J. of Composites for Construction*, 16(4): 430-439.

El-Hacha, R, and Mashrik, MA. 2012. Effect of SFRP confinement on circular and square concrete columns. *Engineering Structures* 36: 379–393.

Fidia srl - Technical Global Services, “FIDSTEEL_3X2-B4_Hardwire” and "FIDSATURANT HM-T", product guide specification, September 2012, web site: http://www.fidiaglobalservice.com.

Mashrik, MA. 2011. Performance evaluation of circular and square concrete columns wrapped with CFRP and SFRP sheets. *M.Sc. Thesis*. University of Calgary, Canada.

Napoli, A, Realfonzo, R. 2011. Strain models for FRP-confined concrete. In: *International RILEM Conference Hong Kong,* September 5-7*,* RILEM Publications S.A.R.L: 568–575.

Napoli, A, Perri, F, Realfonzo, R, and Ruiz Pinilla, JG. 2013. Seismic performance of RC columns strengthened with SFRP systems: experimental study. Submitted to *FRPRCS-11,* Guimarães, June 26-28.

Realfonzo, R, and Napoli, A. 2011. Concrete confined by FRP systems: Confinement efficiency and design strength models. *Composites: Part B,* 42:736–755.

Teng, JG, Chen, JF, Smith, ST, Lam, L. 2002. FRP–strengthened RC structures, Wiley, U.K..